

Hydrostatic pressure effect on archetypal $\text{Sm}_{0.52}\text{Sr}_{0.48}\text{MnO}_3$ single crystal

K. Mydeen,^{1,2} P. Sarkar,^{3,4} P. Mandal,^{4,a)} A. Murugeswari,¹ C. Q. Jin,² and S. Arumugam^{1,b)}

¹Centre for High Pressure Research, School of Physics, Bharathidasan University, Tiruchirappalli 620 024, India

²Beijing National Laboratory for Condensed Matter Physics, Institute of Physics, Chinese Academy of Sciences, Beijing 100 080, People's Republic of China

³Department of Physics, Serampore College, Serampore 712 201, India

⁴Saha Institute of Nuclear Physics, 1/AF Bidhannagar, Calcutta 700 064, India

(Received 15 March 2008; accepted 16 April 2008; published online 9 May 2008)

The effect of hydrostatic pressure (P) on the c -axis electrical resistivity (ρ_c) and ferromagnetic (FM) transition temperature (T_C) of $\text{Sm}_{0.52}\text{Sr}_{0.48}\text{MnO}_3$ single crystal has been investigated. At $P=0$, the strong hysteretic nature of metal-insulator transition (MIT) and the abrupt decrease of ρ_c by several orders just below T_C suggest that the FM transition is discontinuous in nature. The application of pressure strongly decreases ρ_c , shifts MIT to higher temperature at the rate of 19 K/GPa, and suppresses the hysteresis width. The nature of the FM phase transition would change from discontinuous to continuous at around $P=2.5$ GPa. © 2008 American Institute of Physics.

[DOI: 10.1063/1.2920762]

Perovskite manganites $R_{1-x}A_x\text{MnO}_3$ (R for rare earth ions and A for alkaline earth ions) exhibit a rich variety of phenomena due to the presence of several competitive interactions. The relative strength of these interactions can be changed either by tuning the internal parameters such as doping concentration (x), A -site ionic radius (r_A), and disorder or by using the external perturbations such as magnetic field and pressure, and a surprisingly wide variety of phases emerge. Several studies show that quenched disorder or the local structural variation arising due to the size mismatch between R and A ions is a key factor in determining ferromagnetic (FM) transition temperature (T_C) and the phase diagram as a whole.¹⁻⁴ The magnitude of quenched disorder is determined by the A -site size variance $\sigma^2 = \langle r_A^2 \rangle - \langle r_A \rangle^2$.⁵ Such disorders reduce the carrier mobility and the formation energy for lattice polarons and, thus, truncating the FM phase. The disorder will be large in a system with the rare earth element of smaller ionic radius such as Sm, Eu, Gd, and alkaline earth elements of larger ionic radius such as Sr and Ba. Among these, prototype $\text{Sm}_{1-x}\text{Sr}_x\text{MnO}_3$ with x close to 0.5 shows a very sharp drop in magnetization at FM to paramagnetic (PM) transition, where resistivity changes several orders of magnitudes.⁶⁻¹⁰ This suggests that FM phase is truncated, rendering the transition first order. However, there is no systematic analysis on the nature of the magnetic phase transition in the ambient condition as well as in the presence of external pressure. Pressure is a fundamental thermodynamic variable, which facilitates a controlled volume change associated with thermodynamic phase transition. In manganites, pressure also influences the electrical conducting properties as well as the interaction responsible for ferromagnetism. Thus, pressure is an important parameter to study the phase transition and the scattering phenomena in manganites.

In this letter, the electrical resistivity along c axis and ac susceptibility of $\text{Sm}_{0.52}\text{Sr}_{0.48}\text{MnO}_3$ (SSMO) single crystal are measured as a function temperature for different hydrostatic pressure in order to investigate the sensitivity of the elec-

tronic and magnetic properties on external perturbation. We have chosen this composition because near the half-doping ($x=0.5$), the phase competition is most clearly seen and the disorder is maximum. As the composition is close to charge ordering, the effect of external perturbation on physical properties is expected to be large.

Single crystals of SSMO were grown from polycrystalline rods using an optical floating-zone furnace.¹¹ X-ray powder diffraction, Laue diffraction, scanning electron microscopes, and electron probe microanalysis reveal high purity and crystalline quality. The magnetic properties were studied using a superconducting quantum interference device magnetometer (Quantum Design) and an ac susceptometer. Well-characterized crystal was aligned with a goniometer using Laue diffraction and cut along the ab plane and c axis with typical dimensions of $1.5 \times 1.0 \times 0.8$ mm³ and polished. The electrical resistivity was measured by the four-probe technique using a self-clamp-type hybrid hydrostatic pressure cell, and the pressure was monitored using a manganin resistance device.¹²

The main panel of Fig. 1 shows the temperature dependence of c -axis resistivity (ρ_c) of SSMO crystal at various applied pressures (P). Measurements were done for both heating and cooling cycles but the data for heating cycle only are shown for the clarity. At ambient pressure, ρ_c rapidly increases with decreasing temperature until the metal-insulator transition (MIT) temperature (T_{MI}) is reached. At T_{MI} , ρ_c abruptly drops as much as three orders of magnitude. The MIT in this system is extremely sharp, and the sharpness does not appreciably decrease up to the highest applied pressure. The inset of Fig. 1 shows that the MIT is strongly hysteretic with temperature and the width of the hysteresis reduces with increasing pressure. The appearance of hysteresis between heating and cooling cycles indicates that the FM to PM phase transition in this system is first order in nature.¹³ Thermal hysteresis has also been observed in magnetization, resistivity, and other physical parameters measured as a function of magnetic field (H).¹⁴ With increasing pressure, resistivity decreases and MIT shifts toward higher temperature. Depending on the influence of P on ρ_c , the

a)Electronic mail: prabhat.mandal@saha.ac.in.

b)Electronic mail: sarumugam1963@yahoo.com.

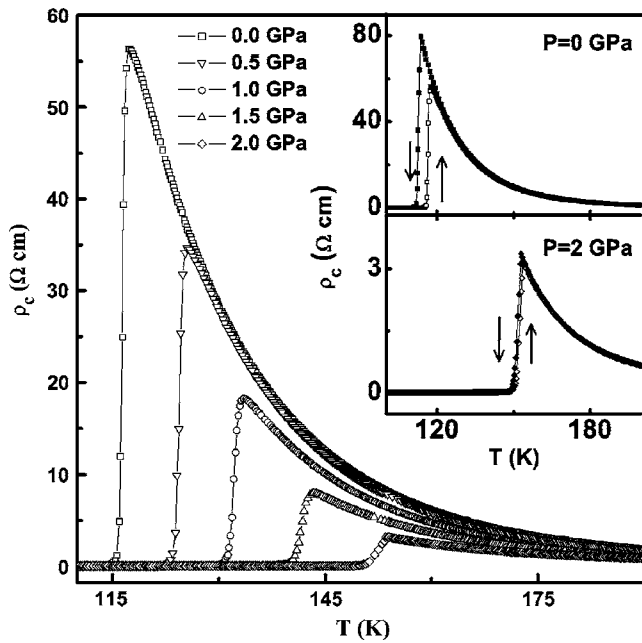


FIG. 1. Temperature dependence of c -axis resistivity (ρ_c) at different pressures for SSMO single crystal. Insets show the thermal hysteresis in ρ_c for $P=0$ and 2.0 GPa.

whole temperature region can be divided into three main parts. At high temperatures well above T_{MI} , the dependence of ρ_c on P is weak, whereas a moderate decrease of ρ_c with P is observed in the FM state. For example, ρ_c at 80 and 300 K decreases with P at the rate of 50 and 18%/GPa, respectively. The effect of pressure on the electrical resistivity is strongest near T_{MI} . The peak resistivity (ρ_p) almost exponentially decreases with pressure.

As MIT in manganites is accompanied by a FM-PM phase transition, we have also investigated the temperature dependence of ac susceptibility (χ) for different pressures to determine the dependence of Curie temperature (T_C) on P . Figure 2(a) shows $\chi(T)$ for SSMO crystal under various pressures. With increasing P , $\chi(T)$ curves shift to the high temperature side. The rapid increase of χ just below T_{MI} indicating that MI and FM-PM transition temperatures are close to each other. The thermal hysteresis of magnetization at ambient pressure is shown in Fig. 2(b). We define the inflection point of $\chi(T)$ curve as T_C and plotted T_C against P in Fig. 2(c). T_C so determined is only few Kelvin lower than that of T_{MI} . T_C increases linearly with P and reveals the value of pressure coefficient $d \ln T_C / dP = 0.15$ K/GPa.

To capture the salient features of electronic conduction and magnetic phase transition in presence of external pressure, it is important to determine the pressure dependence of transport parameters. In Fig. 3, we have plotted different physical parameters as a function of pressure. T_{MI} linearly increases with P at the rate of (dT_{MI}/dP) 19 K/GPa up to the maximum value of applied pressure [Fig. 3(a)]. In several manganites, a linear increase of T_{MI} with P has been observed in the low-pressure regime.^{15–17} The value of dT_{MI}/dP is fairly high in comparison to that found in several wideband manganites but comparable to that observed in narrowband manganites such as $\text{La}_{0.75}\text{Ca}_{0.25}\text{MnO}_3$ (LCMO) and $\text{Pr}_{1-x}\text{Ca}_x\text{MnO}_3$.^{17–21} Figure 3(b) shows the dependence of hysteresis width (ΔT_{MI}) on applied pressure. In the measured pressure range, ΔT_{MI} almost linearly decreases at the

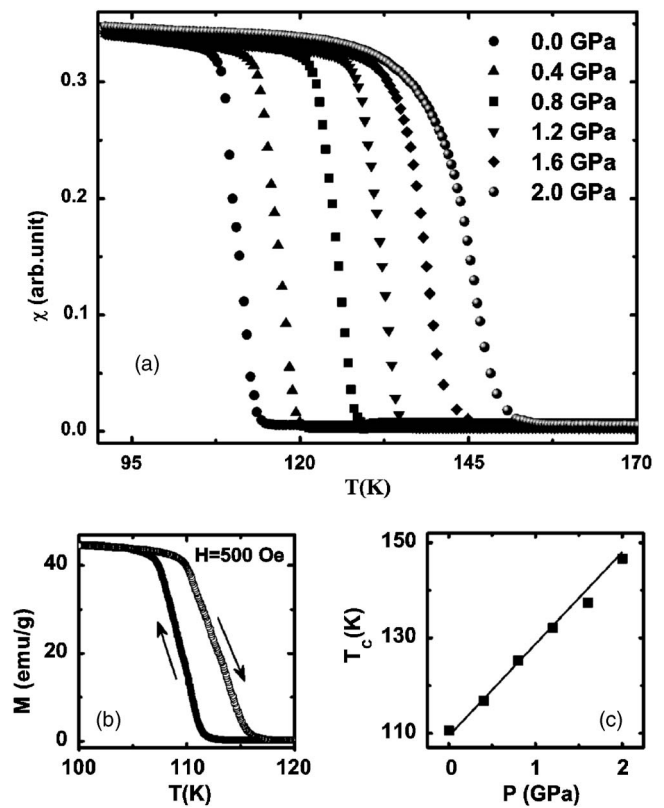


FIG. 2. (a) Temperature dependence of ac susceptibility (χ) at different pressures for SSMO single crystal. (b) The thermal hysteresis of dc magnetization (M) at ambient pressure. (c) The pressure dependence of T_C determined from ac susceptibility.

rate of 1.7 K/GPa. If both T_{MI} and ΔT_{MI} continue to change linearly with P in the same fashion then the hysteresis in $\rho_c(T)$ will disappear above $P=2.5$ GPa and the corresponding value of T_{MI} would be ~ 162 K. A decrease of hysteresis width is also observed in magnetization and resistivity with H . ΔT_{MI} linearly decreases with H at the rate of 1.2 K/T and vanishes above 4 T for T_{MI} close to 162 K.¹⁴ Indeed, the detailed analysis of field dependence of magnetization, resistivity and specific heat shows that the nature of FM to PM transition changes from first order to second order around 4 T.¹⁴ This implies that whether the external perturbation is magnetic field or hydrostatic pressure, the nature of FM transition changes from first order to second order for T_{MI} above

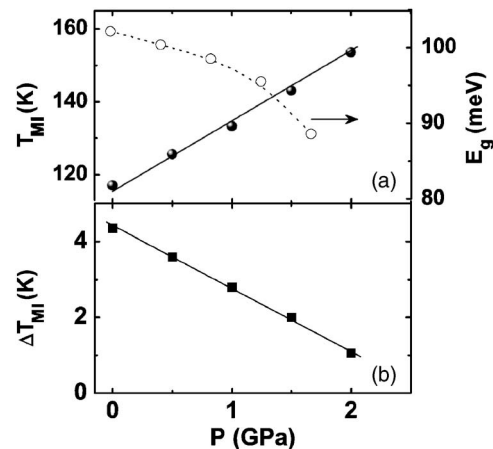


FIG. 3. Pressure dependence of different physical parameters derived from $\rho_c(T)$ curves: (a) T_{MI} and E_g and (b) ΔT_{MI} for SSMO single crystal.

162 K. Thus, as long as the nature of phase transition is concerned a pressure of 2.5 GPa is equivalent to 4 T magnetic field. The effect of pressure and magnetic field on $\rho_c(T)$ are similar close to T_{MI} only. According to the double-exchange theory, the effective transfer interaction (t), which stabilizes the FM metallic phase is given by $t=t_0 \cos(\Delta\theta/2)$, where $\Delta\theta$ is the relative angle between the local t_{2g} spins. t increases mainly due to the increase of $\langle \text{Mn-O-Mn} \rangle$ bond angle and the decrease of Mn-O bond length with the application of pressure. The influence of P on t is large when the bond angle is smaller than 180° . The large value of dT_{MI}/dP in SSMO is partly due to the considerable deviation of this bond angle from 180° .

We would like to compare and contrast the present result on SSMO with the narrowband LCMO. Although the A -site average ionic radius which determines the bandwidth is almost same for both the systems, T_C for LCMO is about 2.5 times higher than that of SSMO. Due to the large ionic size mismatch between Sm and Sr ions, the value of quenched disorder in SSMO ($\sigma^2 \sim 10^{-2} \text{ \AA}^2$) is much larger than that of LCMO ($\sigma^2 \sim 10^{-4} \text{ \AA}^2$). For a system where the A -site chemical disorder is large, the formation energy for lattice polarons is considerably lowered, and when these polarons form in the FM state the ferromagnetism is truncated, rendering the transition first order.³ The huge reduction of T_C and notably sharp MIT along with hysteresis in SSMO are consistent with this picture. It has been claimed that the sharp FM transition may also originate from the coupling of two order parameters.²² Application of pressure reduces local Jahn-Teller distortion and stabilizes the metallic phase; thus, both the conductivity and T_C are enhanced. Other than bandwidth, pressure sensitivity is high for materials having larger local disorder. For quantitative understanding, we have analyzed the temperature dependence of resistivity for different pressures. In the temperature range $T_{MI} < T < 230 \text{ K}$, ρ_c shows an activated behavior $\rho_c \sim \exp[E_g/kT]$, where E_g is the activation energy. The monotonic decrease of E_g from 102 meV at $P=0$ to 89 meV at $P=2.0 \text{ GPa}$, suggests that external pressure suppresses the formation of polaronic state [Fig. 3(a)].

In manganites, it is a well known phenomenon that T_C rapidly increases with the increase of A -site average ionic radius $\langle r_A \rangle$. The increase of T_{MI} with the increase of external pressure and ionic size led to formulate an empirical relation between P and $\langle r_A \rangle$ over a wide range of $\langle r_A \rangle$. It has been shown that the same amount of change in T_{MI} can be achieved by varying either the average ionic radius by $\Delta\langle r_A \rangle$ or the pressure by an amount $\Delta P = \Delta\langle r_A \rangle / \beta$, where the scaling factor β is $3.7 \times 10^{-3} \text{ \AA/GPa}$.¹⁹ The pressure dependence of T_{MI} in manganites has been analyzed using different models.^{21,23} Postorino *et al.* studied the dependence of T_{MI} on applied pressure for LCMO up to 11.2 GPa and shown that T_{MI} follows an empirical relation $T_{MI}(P) = T_\infty - [T_\infty - T_{MI}(0)] \exp(-P/P^*)$, where T_∞ and P^* are known constants.²¹ The explicit dependence of T_{MI} on $\langle r_A \rangle$ was then determined by using the scaling relation $P = \Delta\langle r_A \rangle / \beta$. This relation describes well the P and $\langle r_A \rangle$ dependence of T_{MI} for the manganites with intermediate electron-phonon coupling (EPC) strength but fails in the weak EPC regime. The phase

diagram based on this relation suggests that both SSMO and LCMO should have comparable MIT temperatures. This implies that the simple scaling relation does not hold for SSMO. Also, one can uniquely determine dT_{MI}/dP from the value of T_{MI} of the system. Again, the observed dT_{MI}/dP for SSMO deviates considerably from the one ($\sim 55 \text{ K/GPa}$) deduced from the correlation between dT_{MI}/dP and T_{MI} . It was pointed out that such a deviation may occur when σ^2 is larger than the mean-square thermal displacement of A -site ions.²¹

In conclusion, we have studied the influence of hydrostatic pressure on transport and magnetic properties of SSMO single crystal. At ambient pressure, the sharp magnetic transition, huge drop in resistivity, and thermal hysteresis are the signatures of first-order FM-PM transition. Pressure strongly suppresses local disorder and stabilizes metallic phase, and thus, ρ_c rapidly decreases, T_{MI} shifts to higher temperature, and the thermal hysteresis narrows progressively with increasing pressure. It appears that the characteristic features of first-order transition will disappear above a critical value of applied pressure ($\sim 2.5 \text{ GPa}$), and the transition would be second order in nature.

¹E. Dagotto, T. Hotta, and A. Moreo, *Phys. Rep.* **344**, 1 (2001).

²Y. Tomioka and Y. Tokura, *Phys. Rev. B* **70**, 014432 (2004).

³T. J. Sato, J. W. Lin, and B. Dabrowski, *Phys. Rev. Lett.* **93**, 267204 (2004).

⁴P. Mandal and B. Ghosh, *Phys. Rev. B* **68**, 014422 (2003).

⁵L. M. Rodriguez-Martinez and J. P. Attfield, *Phys. Rev. B* **54**, R15622 (1996); **63**, 024424 (2000).

⁶C. Martin, A. Maignan, M. Hervieu, and B. Raveau, *Phys. Rev. B* **60**, 12191 (1999).

⁷N. A. Babushkina, E. A. Chistotina, O. Yu. Gorbenko, A. R. Kaul, D. I. Khomski, and K. I. Kugel, *Phys. Rev. B* **67**, 100410 (2003).

⁸Y. Endoh, H. Hiraka, Y. Tomioka, Y. Tokura, N. Nagaosa, and T. Fujiwara, *Phys. Rev. Lett.* **94**, 017206 (2005).

⁹A. N. Styka, Y. Ren, O. Yu. Gorbenko, N. A. Babushkina, and D. E. Brown, *J. Appl. Phys.* **100**, 103520 (2006).

¹⁰Y. Tomioka, H. Hiraka, Y. Endoh, and Y. Tokura, *Phys. Rev. B* **74**, 104420 (2006); A. Hassen and P. Mandal, *J. Appl. Phys.* **101**, 113917 (2007).

¹¹P. Mandal, B. Bandyopadhyay, and B. Ghosh, *Phys. Rev. B* **64**, 180405R (2001).

¹²K. Mydeen, S. Arumugam, and C. Q. Jin (unpublished).

¹³S. W. Biernacki, *Phys. Rev. B* **68**, 174417 (2003).

¹⁴P. Sarkar and P. Mandal, *Appl. Phys. Lett.* **92**, 052501 (2008); P. Sarkar and P. Mandal (unpublished).

¹⁵V. Laukhin, J. Fontcuberta, J. L. Garcia-Munoz, and X. Obradors, *Phys. Rev. B* **56**, R10009 (1997); J. Fontcuberta, V. Laukhin, and X. Obradors, *Appl. Phys. Lett.* **72**, 2607 (1998).

¹⁶I. V. Medvedeva, Y. S. Bersenev, K. Bärner, L. Haupt, P. Mandal, and A. Poddar, *Physica B* **229**, 194 (1997).

¹⁷Y. Moritomo, A. Asamitsu, and Y. Tokura, *Phys. Rev. B* **51**, 16491 (1995).

¹⁸J. Neumeier, M. F. Hundley, J. D. Thompson, and R. H. Heffner, *Phys. Rev. B* **52**, R7006 (1995).

¹⁹H. Y. Hwang, T. T. M. Palstra, S. W. Cheong, and B. Batlogg, *Phys. Rev. B* **52**, 15046 (1995).

²⁰C. Cui and T. A. Tyson, *Phys. Rev. B* **70**, 094409 (2004).

²¹P. Postorino, A. Congeduti, P. Dore, A. Sacchetti, F. Gorelli, L. Ulivi, A. Kumar, and D. D. Sarma, *Phys. Rev. Lett.* **91**, 175501 (2003).

²²J. Koscinski, *Theory of Symmetry Changes at Continuous Phase Transitions* (Elsevier, Amsterdam, 1983), p. 1; K. H. O. Bärner and E. A. Zavadskii, *Induzierte magnetische Zustände* (Shaker, Aachen, 2007), p. 189.

²³K. Bärner, I. V. Medvedeva, and E. A. Zavadskii, *Physica B* **355**, 134 (2005).